

Ultrafast Dynamics of the Low-Lying $^3\text{MLCT}$ States of $[\text{Ru}(\text{bpy})_2(\text{dppp2})]^{2+}$

Yujie Sun, Yao Liu, and Claudia Turro*

Department of Chemistry, The Ohio State University, Columbus, Ohio 43210

Received February 28, 2010; E-mail: turro@chemistry.ohio-state.edu

The charge transfer process is a pivotal step in the conversion of photons into electrical and chemical energy in dye-sensitized solar cells and other devices for artificial photosynthesis.¹ The detailed understanding of the initial steps after the absorption of a photon by the dye of a solar cell, typically a mononuclear transition metal complex, is of fundamental importance.¹ The excited state dynamics of organic molecules are well understood and can usually be predicted from rules that relate the rate constants of internal conversion, intersystem crossing, fluorescence, and phosphorescence to various properties, such as Kasha's rule.² In contrast, with the exception of $[\text{Ru}(\text{bpy})_3]^{2+}$ and its structural analogues,^{3,4} a fundamental understanding of the ultrafast excited state processes of transition metal complexes is still lacking. Of particular interest are systems that, unlike organic molecules, possess two populated low-lying triplet excited states that are in fast equilibrium, as described below.

Since the report of the "DNA light-switch" complex $[\text{Ru}(\text{bpy})_2(\text{dppz})]^{2+}$ (**1**, bpy = 2,2'-bipyridine, dppz = dipyrido[3,2-*a*:2',3'-*c*]phenazine, Figure 1), numerous complexes of the type $[\text{Ru}(\text{bpy})_2(\text{L})]^{2+}$ (L = dppz derivative) and $[\text{Ru}(\text{phen})_2(\text{L})]^{2+}$ (phen = 1,10-phenanthroline) have been investigated.⁵ The temperature dependence of the luminescence of **1** in various solvents is consistent with the presence of at least two low-lying $^3\text{MLCT}$ (MLCT = metal-to-ligand charge transfer) states, where a non-emissive or weakly emissive state, $^3\text{MLCT}^{\text{dis}}$, is located at lower energy than the emissive $^3\text{MLCT}^{\text{prox}}$ state. In $^3\text{MLCT}^{\text{dis}}$, the transferred electron is localized on the portion of the dppz ligand distal to the metal, whereas, in $^3\text{MLCT}^{\text{prox}}$, the electron is localized on orbitals of the same ligand proximal to the ruthenium center, making the latter similar to the lowest $^3\text{MLCT}$ state of $[\text{Ru}(\text{bpy})_3]^{2+}$.^{6,7}

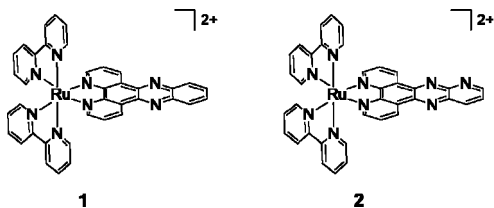


Figure 1. Molecular structures of **1** and **2**.

The solvent dependence of the luminescence of $[\text{Ru}(\text{bpy})_2(\text{dppp2})]^{2+}$ (**2**, dppp2 = pyrido[2',3':5,6]pyrazino[2,3-*f*][1,10]phenanthroline; Figure 1) was recently investigated, where dppp2 is a ligand structurally related to dppz.⁸ The emission maximum of **2** exhibits a large shift from 752 nm in CH_3CN to 653 nm in CH_2Cl_2 (Figure S1), along with an increase in quantum yield from 0.002 to 0.038, attributed to the stabilization of the $^3\text{MLCT}^{\text{dis}}$ state of **2** with solvent polarity.⁸ In contrast, there is a relatively small shift of the emission maximum of **1** from CH_3CN (631 nm) to CH_2Cl_2 (614 nm). The difference in behavior of **1** and **2** is attributed to the emission stemming from $^3\text{MLCT}^{\text{prox}}$ in the former and $^3\text{MLCT}^{\text{dis}}$ in the latter.

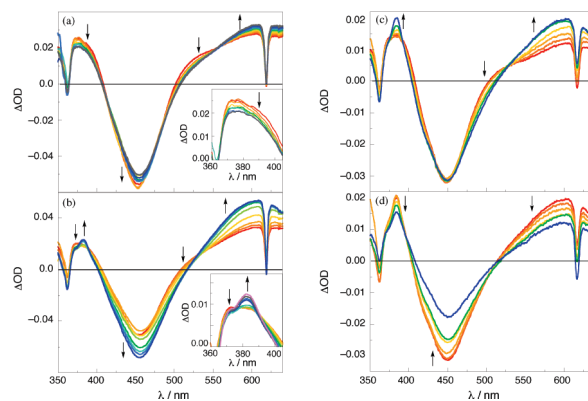


Figure 2. Transient absorption spectra of **2** in CH_3CN (a) 0.35–1.6 ps and (b) 1.6 ps–1 ns and in $\text{CH}_3\text{CH}_2\text{OH}$ (c) 1.6–50 ps and (d) 50 ps–2 ns ($\lambda_{\text{exc}} = 310$ nm, fwhm = 300 fs). Insets in (a) and (b): expanded region from 360 to 405 nm.

Ultrafast techniques were used to elucidate the nature of the excited state manifold of **1**; however, the $^3\text{MLCT}^{\text{dis}}$ state was not well resolved.⁷ The transient absorption spectrum of **1** consists of a strong ground state bleach at 452 nm, a relatively intense bpy^- absorption at 375 nm, and a broad positive signal at $\lambda > 500$ nm (Figure S2). The kinetics of the signal are consistent with changes at early times ($t < 10$ ps) previously attributed in $[\text{Ru}(\text{bpy})_3]^{2+}$ to a combination of intersystem crossing, vibrational cooling, and internal conversion (Figure S2a).³ Relatively minor spectral changes are observed from 10 ps to 1 ns (Figure S2b). The spectral features of **1** at $t > 10$ ps are similar to those assigned as arising from the emissive state, $^3\text{MLCT}^{\text{prox}}$, in $[\text{Ru}(\text{phen})_2(\text{dppz})]^{2+}$, with $\tau = 660$ ns in CH_3CN .^{7a} The transient absorption spectra of **1** in CH_2Cl_2 and $\text{CH}_3\text{CH}_2\text{OH}$ (Figure S3) are similar to those measured in CH_3CN , consistent with the relative invariance of the emission maximum (614–632 nm) and emission lifetime of **1** in these solvents. These results also suggest that the energies of the two low-lying $^3\text{MLCT}$ states of **1** in CH_3CN , CH_2Cl_2 , and $\text{CH}_3\text{CH}_2\text{OH}$ remain relatively constant.

Unlike **1**, the formation of $^3\text{MLCT}^{\text{dis}}$ from $^3\text{MLCT}^{\text{prox}}$ is observed for **2** in the picosecond time scale in CH_3CN . At early times ($t \leq 1.6$ ps), the transient absorption spectra of **2** are similar to those of **1** and $[\text{Ru}(\text{bpy})_3]^{2+}$, with a strong ground state bleach at 454 nm, an intense bpy^- absorption at 373 nm, and a broad and positive absorption band at $\lambda > 500$ nm (Figure 2a). These spectral features are consistent with the population and vibrational cooling of $^3\text{MLCT}^{\text{prox}}$ and result in an isosbestic point at early times at 558 nm (Figure 2a).³ At later times (1.6 ps to 1 ns), there is an increase in the absorption at 606 nm, a decrease of the signal at 373 nm ($\tau = 1.8$ ps), an increase of a sharp feature at 382 nm ($\tau = 30$ ps), and a more intense ground state bleach signal, resulting in a new isosbestic point at 532 nm (Figure 2b). The kinetics measured at each isosbestic point, 532 and 558 nm, can be fitted to ~ 1 and 27 ps, respectively. The signal at 606 nm can be fitted to a biexpo-

nential function with $\tau_1 = 1.5$ ps and $\tau_2 = 21$ ps. The short component is attributed to a combination of intersystem crossing, solvent reorganization, and vibrational cooling of ${}^3\text{MLCT}^{\text{prox}}$, consistent with reports for related complexes, with $\tau \approx 1.5$ ps.³ An increase in the transient absorption signal at 610 nm has been previously attributed to the formation of the ${}^3\text{MLCT}^{\text{dis}}$ state in the related complex $[(\text{bpy})_2\text{Ru}(\text{tpphz})\text{Ru}(\text{bpy})_2]^{4+}$ (tpphz = tetrapyrido[3,2-*a*:3',2'-*c*:3'',2''-*h*:2''',3'''-*j*]phenazine), where the transferred electron is localized on the central part of the bridging tpphz ligand.⁹ Based on the comparison to this work, together with the isosbestic point at 532 nm, the absorption peaks at 382 and 606 nm are assigned to the ${}^3\text{MLCT}^{\text{dis}}$ state in **2**, which is formed from the initially generated ${}^3\text{MLCT}^{\text{prox}}$ with an average rise time of 26 ps. The intensity of the ${}^3\text{MLCT}^{\text{dis}}$ signal begins to plateau at 200 ps and remains constant up to the instrumental limit of 2 ns, consistent with the emission lifetime of **2** in CH_3CN , 35 ns.⁸

The ${}^3\text{MLCT}^{\text{dis}}$ state is expected to be more sensitive to the polarity of the surrounding medium than ${}^3\text{MLCT}^{\text{prox}}$, resulting from the greater dipole moment of the former compared to that of the latter. Therefore, the energy difference between the two states is expected to vary as a function of solvent polarity, thus affecting the rate of interconversion from ${}^3\text{MLCT}^{\text{prox}}$ to ${}^3\text{MLCT}^{\text{dis}}$.⁹ The transient absorption spectrum of **2** in CH_2Cl_2 is similar to that in CH_3CN , with a blue shift of the absorption to 575 nm and slower kinetics (Figures S4). The blue shift is consistent with the reduced stabilization and higher energy of ${}^3\text{MLCT}^{\text{dis}}$ in the less polar medium.⁹ Two kinetic components are observed, one fitted to $\tau \approx 3$ ps at various wavelengths and a rise time of 67 ps measured at 575 nm. Therefore, the interconversion rate from ${}^3\text{MLCT}^{\text{prox}}$ to ${}^3\text{MLCT}^{\text{dis}}$ is slower in CH_2Cl_2 than in CH_3CN by a factor of 2.6, which can be explained by the decreased driving force for the process in the less polar environment.⁹

The luminescence of **1** is sensitive to deactivation by hydrogen bonding in protonated solvents, such as $\text{CH}_3\text{CH}_2\text{OH}$.^{5,6} In contrast to **1** in $\text{CH}_3\text{CH}_2\text{OH}$ and **2** in CH_2Cl_2 and CH_3CN , emission was not detected for **2** in $\text{CH}_3\text{CH}_2\text{OH}$ at room temperature. Figure 2c displays the transient absorption spectrum of **2** in $\text{CH}_3\text{CH}_2\text{OH}$ from 1.6 to 50 ps, showing an increase of a sharp peak at 384 nm and broad absorption at ~ 605 nm with a rise time of 6.7 ps (spectra at $t < 1.6$ ps parallel those in CH_3CN and CH_2Cl_2 and are shown in Figure S5). However, unlike the kinetics of **2** in CH_3CN (Figure 2b) and CH_2Cl_2 (Figure S3b), the signals at 384 nm and ~ 605 nm decay with a lifetime of 1.7 ns in $\text{CH}_3\text{CH}_2\text{OH}$ (Figure 2d).¹⁰ It is apparent from the data in Figure 2c and 2d that both the interconversion of ${}^3\text{MLCT}^{\text{prox}}$ to ${}^3\text{MLCT}^{\text{dis}}$ and the nonemissive decay of the latter to the ground state of **2** are significantly faster in $\text{CH}_3\text{CH}_2\text{OH}$ than in CH_3CN and CH_2Cl_2 . Hydrogen bonding of the noncoordinated nitrogen atoms of the dppp2 ligand to $\text{CH}_3\text{CH}_2\text{OH}$ may result in the greater stabilization of the ${}^3\text{MLCT}^{\text{dis}}$ state of **2** in $\text{CH}_3\text{CH}_2\text{OH}$ than in aprotic solvents.^{5,6} However, a kinetic effect of hydrogen bonding cannot be ruled out at this time.

The Jablonski diagrams of **2** in CH_2Cl_2 , CH_3CN , and $\text{CH}_3\text{CH}_2\text{OH}$ are schematically compared in Figure 3. The energies of the ground state, ${}^1\text{GS}$, and ${}^3\text{MLCT}^{\text{prox}}$ are kept constant in the figure, showing the relative changes to the energy of ${}^3\text{MLCT}^{\text{dis}}$ as a function of solvent. The emission lifetime of **2** was used as the decay of ${}^3\text{MLCT}^{\text{dis}}$ in CH_2Cl_2 and CH_3CN .⁸ It should also be noted that the spectral and kinetic changes observed for **1** in the three solvents (Figures S2 and S3) are relatively small compared to those of **2**, with no significant changes at $t \geq 10 - 20$ ps.

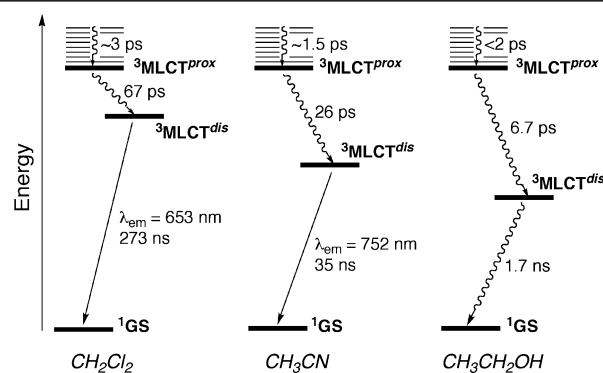


Figure 3. Jablonski diagrams of **2** in CH_2Cl_2 (left), CH_3CN (center), and $\text{CH}_3\text{CH}_2\text{OH}$ (right).

The present work reports the ultrafast generation of the lowest triplet excited state, ${}^3\text{MLCT}^{\text{dis}}$, from the initially populated ${}^3\text{MLCT}^{\text{prox}}$ for **2** in CH_3CN , CH_2Cl_2 , and $\text{CH}_3\text{CH}_2\text{OH}$. The rate of interconversion is highly dependent on solvent polarity and hydrogen bonding. The differences observed for **1** and **2** can be attributed to the lower energy ${}^3\text{MLCT}^{\text{dis}}$ state in the latter, as predicted by the ease of reduction of dppp2 compared to dppz.⁸ This work shows that the rate of interconversion of low-lying triplet excited states in **2** can be tuned by an order of magnitude by solvent stabilization. The findings presented here may be useful in the design of new ruthenium complexes as light-absorbing chromophores and excited state charge transfer relays in solar energy conversion and other applications.

Acknowledgment. C.T. thanks the National Science Foundation (CHE-0911354) and the Center for Chemical and Biological Dynamics (CCBD) at OSU.

Supporting Information Available: Ultrafast spectra of **1** and **2**. This material is available free of charge via the Internet at <http://pubs.acs.org>.

References

- (1) (a) Nocera, D. G. *Chem. Soc. Rev.* **2009**, *38*, 13. (b) Gust, D.; Moore, T. A.; Moore, A. L. *Acc. Chem. Res.* **2009**, *42*, 1890. (c) Wasielewski, M. R. *Acc. Chem. Res.* **2009**, *42*, 1910. (d) Lainé, P. P.; Campagna, S.; Loiseau, F. *Coord. Chem. Rev.* **2008**, *252*, 2552. (e) Hammarstrom, L.; Hammes-Schiffer, S. *Acc. Chem. Res.* **2009**, *42*, 1859.
- (2) Kasha, M. *Faraday Soc. Discuss.* **1950**, *9*, 14.
- (3) (a) Yeh, A. T.; Shank, C. V.; McCusker, J. K. *Science* **2000**, *289*, 935. (b) McCusker, J. K. *Acc. Chem. Res.* **2003**, *36*, 876.
- (4) Liu, Y.; Turner, D. B.; Singh, T. N.; Angeles-Boza, A. M.; Chouai, A.; Dunbar, K. R.; Turro, C. J. *Am. Chem. Soc.* **2009**, *131*, 26.
- (5) (a) Friedman, A. E.; Chambron, J. C.; Sauvage, J. P.; Turro, N. J.; Barton, J. K. *J. Am. Chem. Soc.* **1990**, *112*, 4960. (b) Hartshorn, R. M.; Barton, J. K. *J. Am. Chem. Soc.* **1992**, *114*, 5919.
- (6) (a) Coates, C. G.; Olofsson, J.; Coletti, M.; McGarvey, J. J.; Önfelt, B.; Lincoln, P.; Nordén, B.; Tuite, E.; Matousek, P.; Parker, A. W. *J. Phys. Chem. B* **2001**, *105*, 12653. (b) Brennaman, M. K.; Alstrum-Acevedo, J. H.; Fleming, C. N.; Jang, P.; Meyer, T. J.; Papanikolas, J. M. *J. Am. Chem. Soc.* **2002**, *124*, 15094. (c) Önfelt, B.; Olofsson, J.; Lincoln, P.; Nordén, B. *J. Phys. Chem. A* **2003**, *107*, 1000. (d) Brennaman, M. K.; Meyer, T. J.; Papanikolas, J. M. *J. Phys. Chem. A* **2004**, *108*, 9938.
- (7) (a) Olson, E. J. C.; Hu, D.; Hormann, A.; Jonkman, A. M.; Arkin, M. R.; Stemp, E. D. A.; Barton, J. K.; Barbara, P. F. *J. Am. Chem. Soc.* **1997**, *119*, 11458. (b) Önfelt, B.; Lincoln, P.; Nordén, B.; Baskin, J. S.; Zewail, A. H. *Proc. Natl. Acad. Sci. U.S.A.* **2000**, *97*, 5708.
- (8) Sun, Y.; Turro, C. *Inorg. Chem.*, submitted.
- (9) Flamigni, L.; Encinas, S.; Barigelli, F.; MacDonnell, F. M.; Kim, K.-J.; Puntoriero, F.; Campagna, S. *Chem. Commun.* **2000**, 1185. (b) Chiorboli, C.; Rodgers, M. A. J.; Scandola, F. *J. Am. Chem. Soc.* **2003**, *125*, 483.
- (10) Signal does not decay completely within the 2 ns instrumental limit.

JA101703W